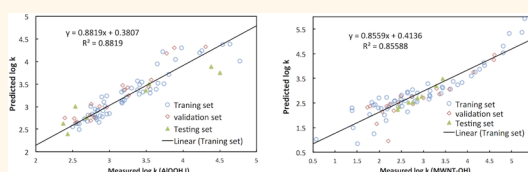# Nanoparticle Surface Characterization and Clustering through Concentration-Dependent Surface Adsorption Modeling

Ran Chen,[†,‡,△] Yuntao Zhang,[†,||,△] Faryad Darabi Sahneh,[†,§] Caterina M. Scoglio,[†,‡,§] Wendel Wohlleben,[⊥] Andrea Haase,[#] Nancy A. Monteiro-Riviere,[‡,||] and Jim E. Riviere[†,||,]*

[†]Institute of Computational Comparative Medicine, [‡]Nanotechnology Innovation Center of Kansas State, [§]Electrical and Computer Engineering Department, and [||]Anatomy and Physiology Department, Kansas State University, Manhattan, Kansas 66506, United States, [⊥]Material Physics GMC, BASF SE 67056 Ludwigshafen, Germany, and [#]Department Chemicals and Product Safety, German Federal Institute for Risk Assessment (BfR), Max-Dohrn-Straße 8-10, 10589 Berlin, Germany. [△]R. Chen and Y. Zhang contributed equally.

ABSTRACT Quantitative characterization of nanoparticle interactions with their surrounding environment is vital for safe nanotechnological development and standardization. A recent quantitative measure, the biological surface adsorption index (BSAI), has demonstrated promising applications in nanomaterial surface characterization and biological/environmental prediction. This paper

further advances the approach beyond the application of five descriptors in the original BSAI to address the concentration dependence of the descriptors, enabling better prediction of the adsorption profile and more accurate categorization of nanomaterials based on their surface properties. Statistical analysis on the obtained adsorption data was performed based on three different models: the original BSAI, a concentration-dependent polynomial model, and an infinite dilution model. These advancements in BSAI modeling showed a promising development in the application of quantitative predictive modeling in biological applications, nanomedicine, and environmental safety assessment of nanomaterials.

KEYWORDS: BSAI · nanoparticles · nanomedicine · nanotoxicology · surface physicochemistry · *in situ* characterization

As the application of nanomaterials in consumer products, industry, and medicine, as well as their presence in the environment, increases, their physicochemical interactions with biological/environmental systems have become one of the most important current cross-disciplinary challenges.[1−3] Nanomaterials' surface physicochemical properties[2,4−10] dictate their environmental and biological impact. Studies on the complexity of such interactions, including electrostatic and hydrophobic interactions, hydrogen bonding, and van der Waals (vdW) forces, have been conducted to better understand the adsorption of biomacromolecules or organic pollutants in the environment. Quantification and standardization of nanomaterials is at the heart of safe, reliable nanotechnological product development. A systematic a pproach of studying physiochemical properties relevant to predicting biological end points is imperatively needed.

The interaction of various molecules with a nanoparticle surface is primarily driven by adsorption energy composed of contributions from several physical or chemical forces such as electrostatic interactions, hydrophobic forces, and hydrogen bonding.[11] We previously defined the biological surface adsorption index (BSAI), consisting of five descriptors obtained from the adsorption measurements of a set of small organic molecules to describe the physicochemical properties of nanomaterial surfaces.[12,13] This aids in understanding the interaction of the particles with either environment-relevant organic molecules or amino acid residues and other functional groups from various biomacromolecules resulting in the formation of a biocorona,[12,13] the latter considered as the determining factor of bioidentity, bioavailability, and toxicity of nanoparticles in biological systems.[14−23] The problem facing quantitative risk assessments in nanosafety applications is that there is no simple experimental approach that can characterize nanoparticle properties that are relevant to biological interactions that modulate nanoparticle

absorption and biodistribution, as well as toxicity once delivered to a target organ. All of these interactions are based on the aforementioned molecular forces that determine solvation and colligative properties in aqueous systems at body temperature, requiring a characterization approach under conditions that mimic this *in vivo* microenvironment. Further advancements in the BSAI would enable this approach to predict the interactions between nanoparticles and large biomacromolecules, which is crucial to predicting both biodistribution and potential mechanisms of toxicity.

BSAI models have shown their capability of characterizing such surface adsorption energy under biologically or environmentally relevant conditions; they are based on the fundamental forces of molecular interactions and can be expressed as[24−26]

$$\log k_i = c + rR_i + p\pi_i + a\alpha_i + b\beta_i + vV_i,$$
$$i = 1, 2, 3, ..., n \qquad (1)$$

where k_i is the adsorption coefficient, n is the number of compounds used as probes, and c is the regression constant. Five variables [R_i, π_i, α_i, β_i, V_i] are the molecular descriptors of the ith probe compound, where R_i is the excess molar refraction representing molecular force of lone-pair electrons, π_i is the polarity/polarizability parameter, α_i and β_i are the hydrogen-bond acidity and basicity, respectively, and V_i is the McGowan characteristic volume describing hydrophobic interactions. The BSAI nanodescriptors are the regression coefficients [r, p, a, b, v] reflecting the differential compound−nanomaterials interactions. Quantitative structure−activity relationship (QSAR) modeling based on molecular connectivity indices was tested and compared to the BSAI approach.[27] It showed slightly better predictive ability; however, the model was not biologically instructive, as it did not illustrate explicitly the relationship between physicochemical properties of nanomaterials and their behavior in a biological or environmental context.

The BSAI model was originally developed at relatively low probe concentrations for nanoparticle characterization, avoiding further influence of probe chemical concentrations with nonlinear adsorption isotherms at higher concentrations. From an experimental perspective, the BSAI nanodescriptors indeed depend on probe concentrations, as the effect of the interactions between molecules of the same species as well as different species became more significant at higher concentrations.[12] In order to better grasp the properties of the surface physicochemistry of the particles and eliminate the concentration effects, the experiments in previous studies were conducted at extremely low probe concentrations. Concentration effects are important for predicting chemical adsorption onto nanomaterials, as there is no control on contaminant concentration in environmental applications. A similar linear free energy relationship (LFER) modeling was performed on adsorption of several

organic molecules onto granular activated carbon, and linear relationships between the regression coefficients and a concentration-related term were discovered at very low concentrations.[28] At higher concentrations, a nonlinear relationship between BSAI nanodescriptors and a concentration term over a broader range of probe concentrations was previously suggested.[12] Second-order polynomial regression between BSAI nanodescriptors and concentration terms was shown to be effective to quantitatively address the probe concentration effects prior to the LFER modeling, especially when applying such a model to the prediction of adsorption of various chemical species of interest.[29] However, a separate regression analysis requires significantly more concentration-dependent adsorption data to ensure the quality of the fitting of the isotherm.

In the current study, different modeling strategies were employed and compared to address this concentration dependence, including the incorporation of a second-order polynomial dependence on concentration-related parameters for each of the nanodescriptors, directly integrated into the BSAI model, as well as a Langmuir model of the adsorption isotherms prior to the application of BSAI (Figure S1). The incorporation of polynomial dependence directly into the original model can utilize experimental data more efficiently, and it does not require additional concentrations to ensure a smooth fit. For the purpose of interpretation of the physicochemical relevance of the model, as well as reducing the possibility of overfitting in cases of a smaller number of test data, an attempt was made to reduce the number of regression coefficients. Based on the polynomial model, less significant factors were then identified through stepwise regression and eliminated from the model. The new model with a reduced number of factors was then further evaluated by cross-validation based on the experimental data. In addition, the predictive ability of the polynomial model was demonstrated by select compounds that have been shown to be environmentally toxic. Lastly, a low-concentration approximation based on the Langmuir adsorption model was employed to extrapolate the adsorption constant at infinite low probe concentration, followed by a regression of the extrapolated constants against molecular descriptors to build a model in an ideal solution to better grasp the physicochemical interactions between the molecules and the surfaces of the particles. A comparison between principal component analysis (PCA) results from the Langmuir infinite dilution model and the original model was made to demonstrate their ability to identify and categorize nanomaterials based on their surface physicochemical properties.

RESULTS

Original BSAI Modeling. Modeling based on our original BSAI approach described by Xia *et al.*[12] was performed on adsorption data of all nanomaterials. Figure S2a
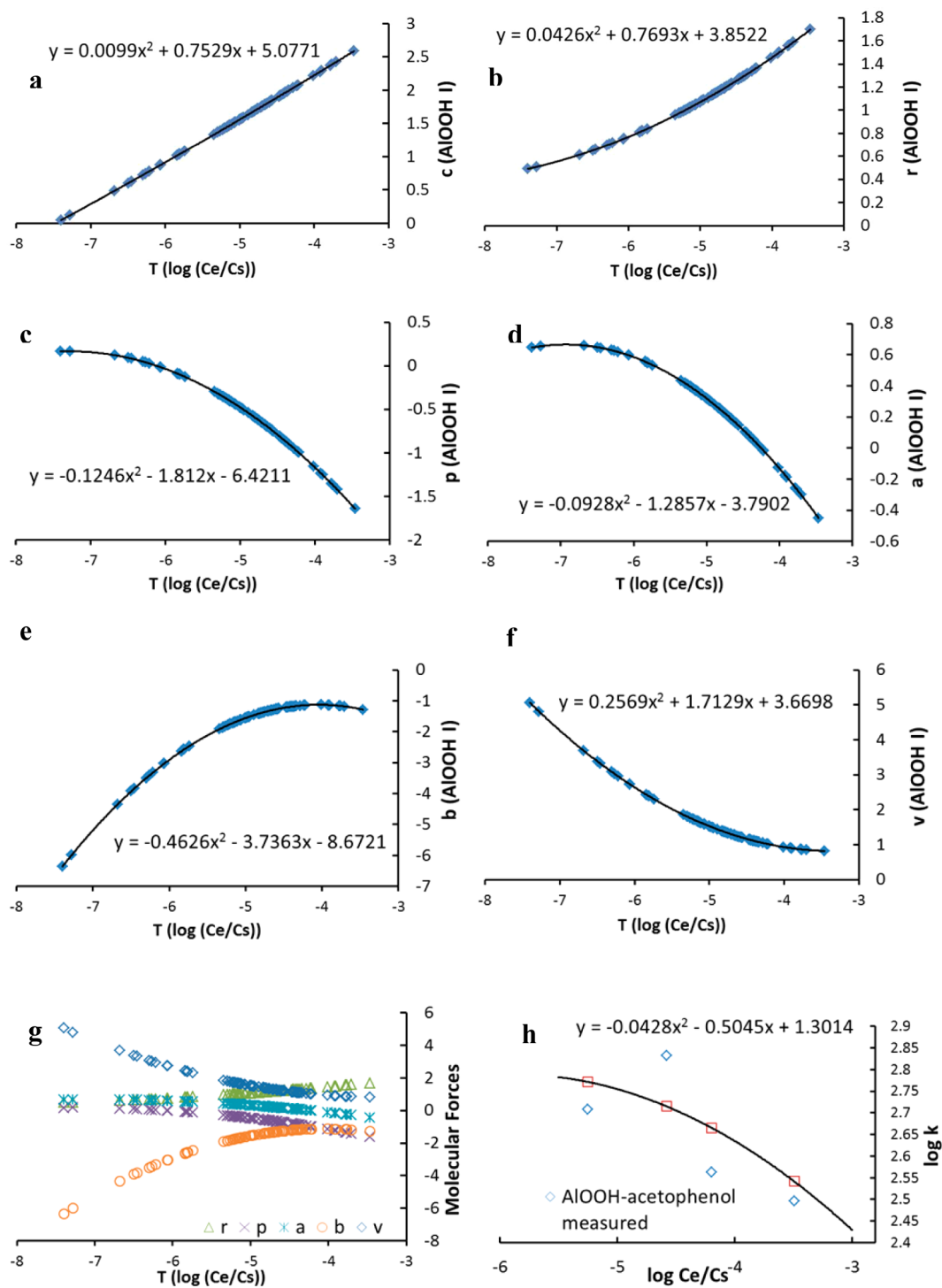
Figure 1. Dependence of nanodescriptors of AlOOH I on probe concentration. Data obtained from a modified model were shown to be polynomial functions of $T = \log(C_e/C_s)$: (a) regression constant c; (b) nanodescriptor r of the excess molar refraction R; (c) nanodescriptor p of the effective solute dipolarity and polarizability π; (d) nanodescriptor a of the effective solute hydrogen-bond acidity α; (e) nanodescriptor b of the effective solute hydrogen-bond basicity β; (f) nanodescriptor v of the McGowan characteristic volume V; (g) comparison of the dependences on concentration among the descriptors; (h) concentration dependence on predicted log k follows a quadratic polynomial function (AlOOH I—acetophenol).

shows the five nanodescriptors of AlOOH I nanoparticles generated from regression analysis of adsorption data from a wide range of probe chemicals at the lowest concentration used in this study (W1). The relative strength of the descriptors (a, b, v values significantly

different from 0) indicated that hydrogen bonding and hydrophobic forces have the greatest contributions toward the interactions between organic chemical species and the surface of the particle. The applicability of the model was tested by a Williams plot, Figure S2b,

showing studentized residuals randomly distributed below and above 0 within the range from -2.5σ to 2.5σ, hat values all smaller than $h^* = 0.72$. The model was further tested by randomly splitting the data into a training set to build the model and an external testing set for predictive capabilities. The model built on the training set was also cross-validated by the leave-one-out method. Although the goodness-of-fit was verified by the correlation coefficient $R^2 = 0.86$, both the internal cross-validation ($Q_{cv}^2 = 0.66$) and external testing were less than ideal, as shown in Figure S2c. Regression results from adsorption data at different concentrations indicated that BSAI descriptors have different patterns of dependence on varied chemical probe concentrations, consistent with Xia et al.'s study.[12]

Predictive Concentration-Dependent Model. To elucidate the role of concentration in the interaction between chemical species and nanoparticle surfaces, a modified model that directly incorporates a concentration-related term $T = \log(C_e/C_s)$ (where C_e is the equilibrium concentration of a probe in the solution after adsorption, and C_s is the solubility of the probe; details of the model are described in the Materials and Methods section) was introduced. First regression analysis on the complete set of data was performed. Then the regression coefficients along with $\log(C_e/C_s)$ were used to reconstruct the BSAI index [r, p, a, b, v] using eq 2. The dependences on T are obtained in Figure 1. Apparently the intermolecular forces represented by the five nanodescriptors have different dependences on the probe chemical concentration. Judging by the ranges of those descriptors, the hydrophobic force (v, 0.82−5.06) has the largest positive contribution toward the adsorption, and it decreases as the equilibrium concentration C_e increases. Such a change could be the result of a competitive binding caused by the interactions among nanoparticle surfaces, water molecules, and different organic molecules present in the mixture. For particles with both hydrophobic and hydrophilic sites, when most of the binding happens between the hydrophobic region on the surface of nanoparticles and the hydrophobic moieties of the molecules, the contribution from the term representing hydrophobic force will be relatively larger. As the chemical concentrations increase, the molecules are driven to bind with less hydrophobic sites on the surface of the nanoparticles, which will cause the contribution from the hydrophobic force term to decrease. However, if the concentration is further increased, the density of molecules bound to hydrophobic sites can still be increased possibly due to the reorientation of the particles or even multiple-layer adsorption caused by intermolecular forces, which will lead to an increase of v. Hydrogen-bond basicity (b, −6.35 to −1.14) has a large negative contribution, indicating the surface is less likely to form a hydrogen bond with the probe chemicals through accepting
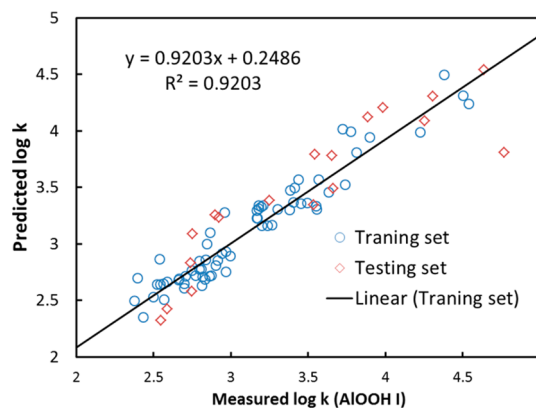

Figure 2. Predicted *versus* measured log k values from AlOOH I. 20% of the total observations were randomly chosen as a testing set; the rest were used to build the model. This figure shows the prediction ability when the training set contains probes at all concentration groups. Training $R^2 = 0.92$ and testing $R^2 = 0.79$.

protons than water molecules. This trend increases as C_e increases possibly because as the proton-accepting ability of the oxygen atom in water molecules is being saturated, the organic molecules are forced to form bonds with surface defects such as oxidation on the surface of the nanoparticles.

Within the concentration range of our experiments, most of the BSAI nanodescriptor−concentration relationships showed obvious nonlinearity, but also a few have very small quadratic terms (*e.g.*, constant c in the case of AlOOH I), which means the concentration dependence of these descriptors can still be described by linear functions relatively well within the respective concentration range. Shih *et al.* proposed a linear relationship to explain the concentration dependence of the descriptors over a different and smaller range of chemical activities (T ranging from −1 to −3) in cases of granular activated carbon. In general their approach was not suitable for the nanosized adsorbent based on our results and previous studies, possibly due to a magnified surface chemical effect caused by significantly higher surface-area-to-mass ratio. But in some cases the polynomial indices may be eliminated to reduce the complexity of our model over the specific range of concentrations in question; such model reduction will be discussed later.

The method was cross-validated by the leave-one-out (LOO) method ($Q_{cv}^2 = 0.83$ for AlOOH I; the rest of the regression coefficients and validation results of some example nanoparticles are listed in Table S1a), as well as external validation by randomly choosing 20% of the entire observations as the testing set and the rest as the training set to build the model (data presented in Table S1b and Figure 2 show measured *versus* predicted for both training set and testing set in the case of AlOOH I, training $R^2 = 0.92$ and testing $R^2 = 0.79$). The applicability of using a set of 17-dimensional indices to make a comparison between
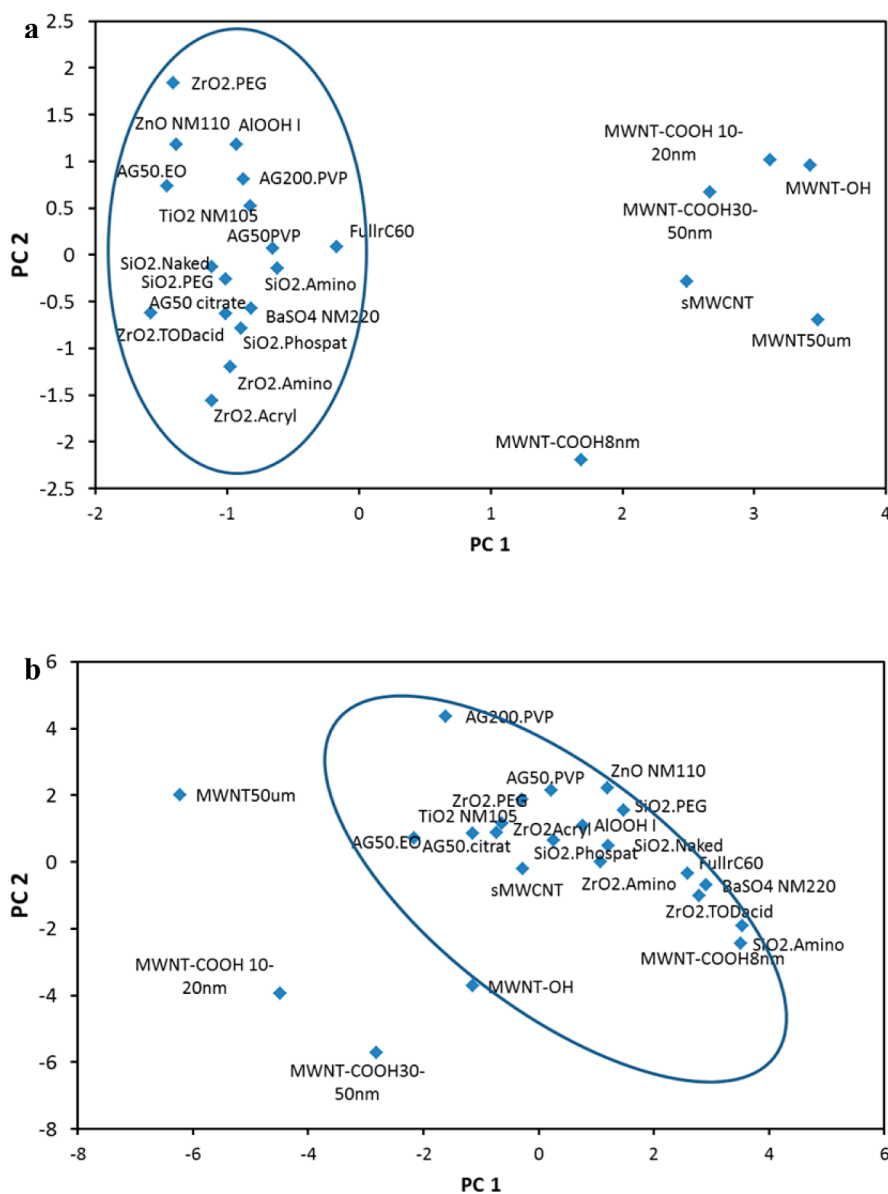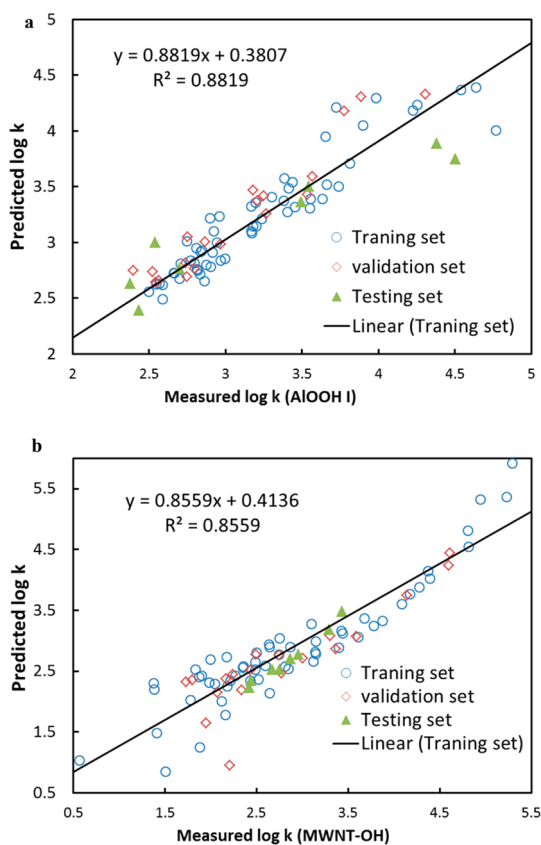
Figure 3. Nanoparticle clustering plots by two principal components. The two components were obtained by principal component analysis of the five nanodescriptors and 17 polynomial indices of both metal/oxide and carbon-based nanoparticles from (a) original BSAI model and (b) polynomial model.

the nanomaterials in terms of surface physicochemical properties was explored by reducing the dimension to two using PCA. PCA mathematically transforms the 17 vectors composed of polynomial indices into a set of new orthogonal vectors, the first two of which account for most of the variance possible and were used to compare between the nanomaterials. Figure 3 clearly demonstrates that both the original BSAI model and the polynomial model are capable of making the separation between metal/oxide and carbon-based nanomaterials. The original BSAI modeling results are included in the Supporting Information for comparison.

In order to further examine the ability of this polynomial model to interpolate to a different concentration that is not used for model building, as well as extrapolate to different compounds, the model was built after data

from the second highest concentration (W10), and two probe compounds that are generally considered as environmental contaminants at four concentration levels (nitrobenzene and chlorophenol) were removed from the training set. For the purpose of model reduction, stepwise regression based on minimal AICc (AICc = AIC + $[(2k(k+1))/(n-k-1)]$, where n is the sample size and k is the number of parameters in the model) was employed for each particle separately, and then the models were manually adjusted to reach possible unification among different nanoparticles. The adsorption data set at the second highest concentration, which was excluded from the training data, was then used as a validation set to examine how well the model built, as previously described, could be used for predicting the adsorption of the compounds at a different concentration; data from
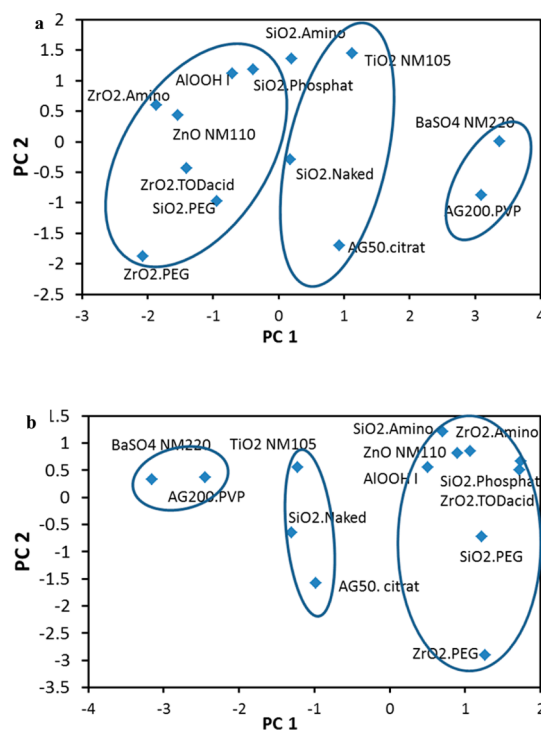
Figure 4. Predicted *versus* measured log *k* values for (a) AlOOH I ($R^2 = 0.86$, $R^2_{validation} = 0.84$, $R^2_{testing} = 0.79$) and (b) MWNT—OH ($R^2 = 0.86$, $R^2_{validation} = 0.75$, $R^2_{testing} = 0.79$).

Figure 5. Nanoparticle clustering plot by two principal components. The two components were obtained by principal component analysis of the five nanodescriptors of metal and oxide nanoparticles from (a) the original BSAI model and (b) the low-concentration approximation by the Langmuir model.

nitrobenzene and chlorophenol were used to test the ability of such a model to predict the adsorption of environmental contaminant chemical compounds. Example results are shown in Table S2: the number of model parameters was reduced to 10 for metal or oxide particles (5 columns on left) and 6 for carbon-based particles (5 columns on right). For most of the particles $R^2 > 0.8$, and validation and testing correlation coefficients ($R^2_{validation}$ and $R^2_{testing}$) are all larger than 0.7. Figure 4 clearly shows successful predictive abilities of the reduced models in cases of AlOOH I ($R^2 = 0.86$, $R^2_{validation} = 0.84$, $R^2_{testing} = 0.79$) and MWNT—OH ($R^2 = 0.86$, $R^2_{validation} = 0.75$, $R^2_{testing} = 0.79$).

Infinite Dilution Adsorption Descriptors. Although the polynomial model shows great potential in terms of its predictive capabilities, the excess indices involved may restrict its application to the interpretation of surface physicochemical properties; therefore only the particles with drastically different surface properties can be clearly distinguished, which in turn may limit its value for providing guidance in nanomaterials engineering and safety assessment. Another approach to address the concentration effect employed here was the low-concentration approximation by the Langmuir model. The probe compound concentration effects are believed to be largely caused by the intertwined interactions between water and compound molecules

and between the same type or different types of molecules,[12,29] since the probability for those interactions to occur increases as the concentration increases. By extrapolating adsorption data to an infinitely low concentration environment, we were able to mimic an ideal aqueous environment, and the true surface chemical physical properties of the nanoparticles, which are not dependent on external factors such as probe concentration, can be exposed, investigated, and compared (Table S3). Figure 5 shows the separation of the metal/oxide nanoparticles by principal components based on regression results using the original BSAI model (Figure 5a, at the lowest concentration) and the Langmuir low-concentration approximation (Figure 5b). A careful comparison between the two revealed that the low-concentration approximation was able to generate the same grouping but with a much better separation between different groups. The polynomial model discussed previously excels in its predictive abilities for both interconcentration and interchemical species predictions; however when applied in the comparison of surface physicochemical properties, it could successfully separate only the carbon-based from the metal/oxide particles, and the distinction within the group of metal/oxides was not detectable. This is possibly because the number of parameters is much larger in the polynomial model, and the errors from multiple dimensions

were confounded when the number of dimensions was reduced to two.

DISCUSSION

The complexity of the adsorption process of chemicals or biomacromolecules onto nanomaterial surfaces arises from the heterogeneity of the particle surface, the molecule functional groups, and the complex environment these materials are exposed to, which govern the nature of interactions that may occur between them. The complexity increases significantly with an increase in concentration, because at higher concentration the competitive interactions between molecules of the same species as well as coexisting different species become extremely complicated. When the BSAI model for the Langmuir low-concentration approximation was built, concentrations of probe chemicals were still required to be experimentally kept as low as possible to make the Langmuir model applicable at that condition.[30] To build a model based on higher concentration measurements, models that consider solute—solute interactions or multilayer adsorption should be employed instead of the Langmuir approach.[30−32] More accurate fittings for isotherms can be achieved by measuring adsorption at smaller concentration intervals. For polynomial models, although concentration is parametrized into the model itself, the application of such a model should still be limited within the concentration range where the dependence on concentration can be properly described as quadratic functions. Other factors that may be incorporated include pH value and temperature. Temperature fluctuations in both biological systems and the environment can significantly alter how the released nanomaterials are transported and transformed and their stability. In principle our model can be extrapolated to include a temperature factor, but certain measures should be employed to avoid excessive variations in temperature, which could cause evaporation of the volatile small organic chemicals. Changes of pH also have realistic relevance since when nanomaterials are transported inside a biological system, they are essentially exposed to environments with different pH values. Such difference would be expected to have a significant impact on our model, especially the first four terms, as they are all based on electron displacement and can be greatly changed when the concentration of protons is changed in the solution. Small organic molecules were used to establish the model because they can be described by relatively simple descriptors and therefore the adsorption by more interpretable models, which is perfect for the sake of surface characterization and categorization of NPs. However, it is indeed a challenge to fit a complex structure such as a large protein to a simple model by reducing its complexity to five descriptors. For such an endeavor to succeed, a much larger data

set would be required to generate a statistically reliable model.

One direct application of the polynomial model would be the prediction of the adsorption of molecules, either contaminants in the environment or biomacromolecules in biological systems. In our experiments, the concentrations of chemicals were still kept low so that the original BSAI model and the Langmuir model can both be applied. In the application to prediction, one must make sure that the concentration used for model building is at least comparable to the concentration of the molecules to be predicted, because if the concentration falls into a completely different region, the model itself might no longer be valid. For the same reason, the probe chemicals used in model building should also be spread out over a range of physicochemical properties whose chemical space is wide enough to cover the target molecule to be predicted.

It is worthy to note that the surface coating of the particles made of the same type of materials can make the adsorption profile significantly different. Opposite signs in the quadratic terms were observed (e.g., SiO_2.Amino and SiO_2.Naked, Figure S3), which would change the trend of dependence on concentrations. This is understandable because the trend is determined by both the number of probe molecules in the solution and the number of active surface adsorption sites. In the cases of SiO_2.Amino and SiO_2.Naked, obviously the amino coating changed drastically in p (interactions from molecule dipolarity and polarizability) and v (hydrophobic forces), which may be attributed to the increased hydrophilic sites caused by the surface coating compared to pristine nanoparticles. Thus, the evaluation of particles engineered with various surface coatings can be achieved.

Since factors other than solely particle surface forces, such as intermolecular interactions among different solutes and water, are largely excluded by the low-concentration approximation of BSAI descriptors, the clustering on those descriptors should be able to more accurately categorize nanomaterials being tested. One possible application would be using several types of particles with different but known biological/environmental behaviors, combining a clustering result with many other unknown particles, to predict the behavior of the unknown. For example, similarly clustered particles should attract similar particular types of proteins. Since the biological impact of nanomaterials is largely determined by their affinity for biomacromolecules including proteins and subcellular structures such as lipid bilayers, materials with the same bioidentity, biodistribution, or toxicity may likely be found within the same cluster.[33]

There are also multiple applications in the field of nanomaterial environmental safety assessment. A BSAI approach would be particularly powerful in

characterizing the bioidentity of complex manufactured nanomaterial structures relative to their environmental safety. As demonstrated by our ability to predict nanomaterial binding to the environmental contaminants nitrobenzene and chlorophenol, knowledge of a nanomaterial's BSAI would allow initial predictions of the material's interactions with contaminants in aqueous environments such as aquifers, surface ponds, and lakes. A more powerful application would be in environmental remediation, where one could define an optimal BSAI with high affinity for a specific contaminant in a defined environment and then, using statistical clustering, identify an appropriate nanomaterial. In order to continue development and application of this index, it will be crucial to correlate BSAI-characterized nanomaterials with known biological and environmental end points.

CONCLUSIONS

In summary, the present study utilized large sets of experimental nanomaterial adsorption data and modified modeling approaches to generate more advanced BSAI models of nanomaterial surface characterization that possess improved predicting and categorizing abilities. We have shown better prediction results from the polynomial models over varied concentration ranges for both interchemical species and interconcentration predictions. Better separation, even among a group of nanomaterials with similar chemical compositions (e.g., metals and oxides), was also achieved by infinite dilution approximation based on Langmuir models. We believe such separation based on core materials physicochemically originated from the possible ionic interactions or chelation effects for metal/oxide and prominent hydrophobic interactions for carbon-based materials. Thus, these improved models can be established as a standardized characterization method aimed at building a database of descriptors from known nanomaterials along with their biorelated test data for the prediction of their bioidentity due to biomolecule adsorption and their possible cellular uptake pathways. Since biological behavior is largely determined by the physicochemical interactions with molecules in biological environments such as serum, plasma, or lung fluids, the models can also be used to identify new nanomaterials that may have similar biological effects including bioidentity, bioavailability, biodistribution, and toxicity by comparing their surface descriptors to those known nanomaterials documented in the database through statistical clustering. With further advancement, such BSAI modeling may be able to be applied in conjunction with pharmacokinetic models to describe or predict the fate of nanomaterials within the whole organism. It has been shown that the improved BSAI approach can provide an *in silico* quantitative safety assessment for nanomaterials and guidelines for the development of novel nanomaterials for diagnostics and therapeutics by targeting specific surface descriptors.

MATERIALS AND METHODS

Nanomaterials and Chemicals. Some of the nanomaterials used in this study (including AlOOH, BaSO$_4$, TiO$_2$, ZnO, SiO$_2$, ZrO$_2$, and Ag) were obtained through the nanoGEM collaboration. Data of the rest of the particles were obtained from studies previously conducted by our group. All chemicals used as probes in this research were purchased from Sigma (St. Louis, MO, USA). Brief physicochemical characteristics of the nanomaterials used are indicated in Table 1, and detailed characterization data of nanoGEM materials can be found in Table S4. The suffixes of the names indicate the chemical composition of surface coatings on metal/oxide particles: Naked means no coating, Amino is a coating of amino groups, PEG is polyethylene glycol, Phosphat means phosphate, Acryl means acrylic acid, TODacid is trioxadecanoic acid, EO is ethylene oxide, Citrat is citrate, and PVP is polyvinlypropylene. The number following the core materials indicates the size (e.g., Ag 50 and Ag 200 are 50 and 200 nm silver particles). NM*x* numbering refers to the respective numbering of OECD reference nanomaterials.[34,35] We also used carbon-based materials including short multi-walled carbon nanotubes (sMWCNTs), fullerene (FullrC60), and multiwalled nanotubes (MWNTs) with surface coatings of either carboxyl (−COOH) or hydroxyl (−OH).

Adsorption of Nanomaterials with Chemical Probes. The adsorption experiments were conducted based on an established protocol by our group with current modifications.[12,13] In brief, 2 mg of nanoparticles was added into a 2 mL glass vial filled with 200 μL of deionized water. The vial was then vortexed to suspend the nanoparticles before 1 mL of working solution (W1, W5, W10, W25, or W50) containing probe compounds of various concentrations was added to the vial. The vial was then sealed immediately with a Teflon-lined septa cap to prevent evaporation of compounds. For nanomaterials in aqueous suspensions, a volume of the aqueous suspensions equal to 2 mg of solid nanomaterial was mixed with the working solution to get the same concentrations as the solid nanomaterials above. The process of adsorption of probe compounds onto nanoparticles was conducted by vigorous shaking of the mixtures for 5 h until an equilibrium condition was reached. The particles were then removed from the solution by centrifugation.

Analysis of Chemical Probes by SPME and GC/MS. Solid phase microextraction (SPME) in combination with gas chromatography mass spectrometry (GC/MS, Agilent GC-QQQ 7000B) was employed to determine the concentration changes of probe components before and after adsorption with nanomaterials. In SPME, a poly(dimethylsiloxane)/divinylbenzene (PDMS/DVB) membrane coated fiber was used for the extraction of probe compounds from the liquid phase. The extraction time was 20 min. In GC/MS, separation was performed on a 30 m × 0.25 mm (i.d.) × 0.25 μm (df) HP-5MS capillary column (Agilent, Palo Alto, CA, USA). The column oven was programmed as follows: the initial temperature was 40 °C and held for 1 min, ramped at 20 °C/min to 60 and 2 °C/min to 100 °C, held at 100 °C for 2 min, then ramped at 20 °C/min to 200 and 40 °C/min to 270 °C, and finally held at 270 °C for 3 min. The injection port was maintained at 280 °C for using PDMS/DVB fibers. The injection model was pulsed/splitless and desorption time was 5 min. An Agilent GC-QQQ/MassHunter workstation was used for data acquisition. The equilibrium concentrations (C_e) were directly determined using Qualitative Analysis software (Agilent). The surface concentration of adsorbed probe compounds was determined as $C_{ad} = (V_0(C_0 - C_e))/m$, where V_0 is the total volume in the vial, C_0 is the concentration of a probe compound prior to adsorption, and m is the mass of nanoparticles

TABLE 1. Physicochemical Characterizations of the Nanomaterials Used in This Study[a]

	diameter (TEM, nm)	diameter (Zetasizer, nm)	zeta-potential (mV)	specific surface area (m²/g)	surface coating
AlOOH I	37	262	5	47	none
BaSO₄ NM220	32	350	−39	41	polymer
TiO₂ NM105	21	478	−17	51	none
ZnO NM110	80		20	12	none
SiO₂.Amino	15	42	0	200	amino
SiO₂.Naked	15	40	−39	200	none/OH
SiO₂.PEG	15	50	−26	200	PEG500
SiO₂.Phosphat	15	40	−42.9	200	phosphonate
ZrO₂.Acryl	9	9	−39	117	acrylic acid COOH polymer
ZrO₂.Amino	10	315	3.9	105	amino
ZrO₂.PEG	9	27	−7.8	117	PEG600
ZrO₂.TODacid	9	9	−6.5	117	troxadecanoic acid
AG50.EO	7	40	−20	86	ethylenoxide
AG50.Citrat	20	35	−45	30	citrate
AG50.PVP	97	123	−7	6.2	polyvinlypropylene
AG200.PVP	134	408	−7	4.5	polyvinlypropylene

	outer diameter (nm)	length (μm)	SSA (m²/g)	purity (wt %)	surface coating (wt %)
sMWCNT	8—15	0.5—2	233	95	
FullrC60	1			98	
MWNT-OH	8—15	~50	233	95	3.7 OH
MWNT50μm	8—15	~50	233	95	
MWNT-COOH 10—20nm	10—20	10—30	233	95	2 COOH
MWNT-COOH8nm	<8	10—30	500	95	3.86 COOH
MWNT-COOH30—50nm	30—50	10—20	60	95	0.73 COOH

[a] Full characterization is available in the Supporting Information.

present in the suspension. The adsorption constant of a given compound onto a particular type of particle is the ratio of surface concentration (C_{ad}) *versus* the equilibrium concentration (C_e):

$$k = \frac{C_{ad}}{C_e} = \frac{V_0(C_0 - C_e)}{mC_e} \qquad (2)$$

Polynomial Modeling. The nanodescriptors for a given nanoparticle were then obtained using multiple linear regression analysis of the [log k,r,p,a,b,v] matrix. The Abraham solute descriptors [R_i, π_i, α_i, β_i, V_i] were generated using the Absolv module provided by ADME online service (Advanced Chemistry Development Inc., Toronto, Canada). The regression analysis was performed by JMP Pro (SAS Institute Inc., Cary, NC, USA). The robustness of the models was tested by internal cross-validation using the leave-one-out technique; typically the model is considered robust when *PRESS RMSE* < 1 and Q_{cv}^2 > 0.7.

A polynomial dependence of nanodescriptors on concentrations is incorporated in the model: $\log k_i = c + rR_i + p\pi_i + a\alpha_i + b\beta_i + vV_i$, $i = 1, 2, 3, ..., n$, where

$$c = lT^2 + mT + n$$

$$r = l_r T^2 + m_r T + n_r$$

$$p = l_p T^2 + m_p T + n_p$$

$$a = l_a T^2 + m_a T + n_a$$

$$b = l_b T^2 + m_b T + n_b$$

$$v = l_v T^2 + m_v T + n_v \qquad (3)$$

$T = \log(C_e/C_s)$, where C_e is the equilibrium concentration of a probe in the solution after adsorption and C_s is the solubility of

the probe; chemical activity = C_e/C_s is used as a parametrized level of chemical saturation in the aqueous phase.

The new regression coefficient becomes [$l, m, n, l_r, ..., m_v, n_v$] (polynomial indices). Here, the indices were directly imbedded in the model when the regression analysis was performed, instead of being used as regression coefficient in a separate second-order polynomial model after the original LFER modeling is finished. Since this polynomial model takes probe chemical concentration into consideration, it is ideally suited for the prediction of the adsorption of various organic chemical species at different concentrations onto nanoparticles.

Infinite Dilution Adsorption Index Based on Langmuir Theory. Adsorption depends both on nanoparticles physiochemical properties and on compound concentrations. In order to isolate the influence of physiochemical properties for nanoparticle characterization, we need to minimize the concentration effects. To do so, theoretically, we can define the adsorption index for infinitesimally small concentrations. Such an index, referred to as *infinite dilution adsorption index* and denoted by k_∞, has the following definition:

$$k_\infty = \lim_{C_0 \to 0} \frac{C_e}{C_{ad}}$$

In the original BSAI model, the theoretical infinite dilution adsorption index is approximately obtained through using very small concentrations. Measurement errors, however, limit the minimum possible concentration in an experimental setup, because the concentration measurements should be distinguishable from the persistent noise. In order to overcome this issue, we alternatively employed an analysis based on the Langmuir adsorption theory.[36] According to Langmuir theory, the relationship between adsorbed concentration and equilibrium concentration is as follows:

$$C_{ad} = \frac{KQC_e}{1 + KC_e}$$

where Q is the maximum possible adsorbed amount as C_e increases, and K is the Langmuir equilibrium constant. At infinitesimally low

concentration, $C_{ad}/C_e \rightarrow QK$, suggesting that $k_\infty = QK$. Therefore, fitting the Langmuir model to experimental measurements provides an estimate of the infinite dilution adsorption index. Importantly, this estimate is not very sensitive to measurement errors, as model fitting over multiple concentrations averages out the errors rather than being solely reliant on estimating a single low concentration.

In this paper, adsorption data from four concentration groups were used for the Langmuir regression in the linearized form: $C_e/C_{ad} = (1/Q)C_e + (1/QK)$. The low-concentration approximation yields adsorption constant k_0 at ideal conditions (infinitely low concentration) by regression between C_e/C_{ad} and C_e. The log k_∞ was used for BSAI modeling in the same manner as the original model to generate concentration-independent nanodescriptors. The model built based on this approximation can be used to characterize and compare surface physicochemical properties of nanomaterials, since the exclusion of probe concentration effect is achieved by the model. The entire process of experimental methods and statistical analysis used to calculate a BSAI index is illustrated by the flowchart in Figure S1.

Conflict of Interest: The authors declare no competing financial interest.

Supporting Information Available: Three supplementary figures and their legends; five supplementary tables and their titles. This material is available free of charge *via* the Internet at http://pubs.acs.org.

REFERENCES AND NOTES

1. Moyano, D. F.; Rotello, V. M. Nano Meets Biology: Structure and Function at the Nanoparticle Interface. *Langmuir* **2011**, *27*, 10376–10385.
2. Ke, P. C.; Lamm, M. H. A Biophysical Perspective of Understanding Nanoparticles at Large. *Phys. Chem. Chem. Phys.* **2011**, *13*, 7273–7283.
3. Mailänder, V.; Landfester, K. Interaction of Nanoparticles with Cells. *Biomacromolecules* **2009**, *10*, 2379–2400.
4. Nel, A. E.; Mädler, L.; Velegol, D.; Xia, T.; Hoek, E. M. V.; Somasundaran, P.; Klaessig, F.; Castranova, V.; Thompson, M. Understanding Biophysicochemical Interactions at the Nano–Bio Interface. *Nat. Mater.* **2009**, *8*, 543–557.
5. Lewinski, N.; Colvin, V.; Drezek, R. Cytotoxicity of Nanoparticles. *Small* **2008**, *4*, 26–49.
6. Verma, A.; Stellacci, F. Effect of Surface Properties on Nanoparticle-Cell Interactions. *Small* **2009**, *6*, 1–10.
7. Chen, R.; Ratnikova, T. A.; Stone, M. B.; Lin, S.; Lard, M.; Huang, G.; Hudson, J. S.; Ke, P. C. Differential Uptake of Carbon Nanoparticles by Plant and Mammalian Cells. *Small* **2010**, *6*, 612–617.
8. Shi, M.; Kwon, H. S.; Peng, Z.; Elder, A.; Yang, H. Effects of Surface Chemistry on the Generation of Reactive Oxygen Species by Copper Nanoparticles. *ACS Nano* **2012**, *6*, 2157–2164.
9. Pasquini, L. M.; Hashmi, S. M.; Sommer, T. J.; Elimelech, M.; Zimmerman, J. B. Impact of Surface Functionalization on Bacterial Cytotoxicity of Single-Walled Carbon Nanotubes. *Environ. Sci. Technol.* **2012**, *46*, 6297–6305.
10. Podila, R.; Chen, R.; Ke, P. C.; Brown, J. M.; Rao, A. M. Effects of Surface Functional Groups on the Formation of Nanoparticle-Protein Corona. *Appl. Phys. Lett.* **2012**, *101*, 263701.
11. Stone, A. *The Theory of Intermolecular Forces*; Oxford University Press, 2013; pp 4–7.
12. Xia, X.-R.; Monteiro-Riviere, N. A.; Riviere, J. E. An Index for Characterization of Nanomaterials in Biological Systems. *Nat. Nanotechnol.* **2010**, *5*, 671–675.
13. Xia, X. R.; Monteiro-Riviere, N. A.; Mathur, S.; Song, X.; Xiao, L.; Oldenberg, S. J.; Fadeel, B.; Riviere, J. E. Mapping the Surface Adsorption Forces of Nanomaterials in Biological Systems. *ACS Nano* **2011**, *5*, 9074–9081.
14. Klein, J. Probing the Interactions of Proteins and Nanoparticles. *Proc. Natl. Acad. Sci. U.S.A.* **2007**, *104*, 2029–2030.
15. Lynch, I.; Salvati, A.; Dawson, K. A. Protein-Nanoparticle Interactions: What Does the Cell See? *Nat. Nanotechnol.* **2009**, *4*, 546–547.
16. Cedervall, T.; Lynch, I.; Lindman, S.; Berggård, T.; Thulin, E.; Nilsson, H.; Dawson, K. A.; Linse, S. Understanding the Nanoparticle–Protein Corona Using Methods to Quantify Exchange Rates and Affinities of Proteins for Nanoparticles. *Proc. Natl. Acad. Sci. U.S.A.* **2007**, *104*, 2050–2055.
17. Laera, S.; Ceccone, G.; Rossi, F.; Gilliland, D.; Hussain, R.; Siligardi, G.; Calzolai, L. Measuring Protein Structure and Stability of Protein–Nanoparticle Systems with Synchrotron Radiation Circular Dichroism. *Nano Lett.* **2011**, *11*, 4480–4484.
18. Sund, J.; Alenius, H.; Vippola, M.; Savolainen, K.; Puustinen, A. Proteomic Characterization of Engineered Nanomaterial-Protein Interactions in Relation to Surface Reactivity. *ACS Nano* **2011**, *5*, 4300–4309.
19. Lynch, I.; Dawson, K. A. Protein-Nanoparticle Interactions. *Nano Today* **2008**, *3*, 40–47.
20. Lynch, I.; Cedervall, T.; Lundqvist, M.; Cabaleiro-Lago, C.; Linse, S.; Dawson, K. A. The Nanoparticle-Protein Complex as a Biological Entity; a Complex Fluids and Surface Science Challenge for the 21st Century. *Adv. Colloid Interface Sci.* **2007**, *134–135*, 167–174.
21. Chen, R.; Choudhary, P.; Schurr, R. N.; Bhattacharya, P.; Brown, J. M.; Ke, P. C. Interaction of Lipid Vesicle with Silver Nanoparticle-Serum Albumin Protein Corona. *Appl. Phys. Lett.* **2012**, *100*, 013703.
22. Chen, R.; Radic, S.; Choudhary, P.; Ledwell, K. G.; Huang, G.; Brown, J. M.; Ke, P. C. Formation and Cell Translocation of Carbon Nanotube-Fibrinogen Protein Corona. *Appl. Phys. Lett.* **2012**, *101*, 133702.
23. Riviere, J. E.; Scoglio, C.; Sahneh, F. D.; Monteiro-Riviere, N. A. Computational Approaches and Metrics Required for Formulating Biologically Realistic Nanomaterial Pharmacokinetic Models. *Comput. Sci. Discovery* **2013**, *6*, 014005.
24. Abraham, M. H. Scales of Solute Hydrogen-Bonding: Their Construction and Application to Physicochemical and Biochemical Processes. *Chem. Soc. Rev.* **1993**, *22*, 73–83.
25. Dehmer, M.; Varmuza, K.; Bonchev, D. *Statistical Modelling of Molecular Descriptors in QSAR/QSPR*; John Wiley & Sons, 2012; pp 65–68.
26. Karelson, M. *Molecular Descriptors in QSAR/QSPR*; Wiley-Interscience, 2000; pp 75–120.
27. Apul, O. G.; Wang, Q.; Shao, T.; Rieck, J. R.; Karanfil, T. Predictive Model Development for Adsorption of Aromatic Contaminants by Multi-Walled Carbon Nanotubes. *Environ. Sci. Technol.* **2013**, *47*, 2295–2303.
28. Shih, Y.-H.; Gschwend, P. M. Evaluating Activated Carbon-Water Sorption Coefficients of Organic Compounds Using a Linear Solvation Energy Relationship Approach and Sorbate Chemical Activities. *Environ. Sci. Technol.* **2009**, *43*, 851–857.
29. Zhao, Q.; Yang, K.; Li, W.; Xing, B. Concentration-Dependent Polyparameter Linear Free Energy Relationships to Predict Organic Compound Sorption on Carbon Nanotubes. *Sci. Rep.* **2014**, *4*, 3888–3888.
30. Ruthven, D. M. *Principles of Adsorption and Adsorption Processes*; John Wiley & Sons, 1984; pp 89–95.
31. Wu, W.; Chen, W.; Lin, D.; Yang, K. Influence of Surface Oxidation of Multiwalled Carbon Nanotubes on the Adsorption Affinity and Capacity of Polar and Nonpolar Organic Compounds in Aqueous Phase. *Environ. Sci. Technol.* **2012**, *46*, 5446–5454.

32. Yang, K.; Xing, B. Adsorption of Organic Compounds by Carbon Nanomaterials in Aqueous Phase: Polanyi Theory and Its Application. *Chem. Rev.* **2010**, *110*, 5989–6008.

33. Aillon, K. L.; Xie, Y.; El-Gendy, N.; Berkland, C. J.; Forrest, M. L. Effects of Nanomaterial Physicochemical Properties on *in Vivo* Toxicity. *Adv. Drug Delivery Rev.* **2009**, *61*, 457–466.

34. Landsiedel, R.; Ma-Hock, L.; Hofmann, T.; Wiemann, M.; Strauss, V.; Treumann, S.; Wohlleben, W.; Gröters, S.; Wiench, K.; van Ravenzwaay, B. Application of Short-Term Inhalation Studies to Assess the Inhalation Toxicity of Nanomaterials. *Part. Fibre Toxicol.* **2014**, *11*, 16.

35. Wohlleben, W.; Kuhlbusch, T. A. J.; Schnekenburger, J.; Lehr, C.-M. *Safety of Nanomaterials along Their Lifecycle: Release, Exposure, and Human Hazards*; Taylor & Francis, 2014; pp 76−84.

36. Masel, R. I. *Principles of Adsorption and Reaction on Solid Surfaces*; John Wiley & Sons, 1996; pp 240−246.